PHYSICAL REVIEW D **82,** 105014 (2010)

Singlet Majorana fermion dark matter, DAMA, CoGeNT, and CDMS-II

C. A. de S. Pires,* F. S. Queiroz,† and P. S. Rodrigues da Silva‡

Departamento de Física, Universidade Federal da Paraíba, Caixa Postal 5008, 58051-970, João Pessoa - PB, Brazil

(Received 4 July 2010; published 16 November 2010)

We propose a model where a sterile Majorana fermion with mass in the range of 10 GeV–1 TeV can account for the whole amount of dark matter in the Universe. The model involves a right-handed singlet Majorana fermion as a weakly interacting massive particle, a charged and a neutral scalar, and all singlets by the standard model symmetry and makes use of a discrete symmetry in order to guarantee the singlet fermion stability. Also, motivated by the recent results reported by CoGeNT and CDMS-II experiments concerning excess events of the expected background, and the intriguing annual modulation observed by DAMA, we look for a possible explanation to some of these experiments. Our results show that there is a lot of room in the parameter space to make this sterile Majorana fermion a viable dark matter candidate, and, if it is realized in nature, it is also capable of explaining DAMA annual modulation signal and/or CoGeNT excess events or CDMS-II excess event candidates. Besides, a light Higgs boson is preferred in this scenario.

DOI: 10.1103/PhysRevD.82.105014 PACS numbers: 12.60.−i, 14.60.St, 14.80.−j, 95.35.+d

I. INTRODUCTION

Dark matter (DM) has become one of the most promising evidences in favor of physics beyond the standard model of electroweak interactions (SM). The converging paradigm to naturally explain this unseen component of matter is that it be a weakly interacting massive particle (WIMP), with a mass scale ranging from tens of GeV to a few TeV [1]. With recent data from the Wilkinson Microwave Anisotropy Probe (WMAP) [2] and several DM direct detection experiments running and projected [3–6], we have powerful new tools to investigate particle physics models which just provide new particle content that would explain this dark component. Besides, the Large Hadron Collider (LHC) is already running [7] and may be able to shed some light on the DM component, too.

One of the known particles that could provide some link to the DM problem is the neutrino. Remember, though, that active neutrinos are underweight to satisfy this picture, since their density parameter Ω_ν is given by [8]

$$\Omega_\nu h^2 = \frac{\sum m_\nu}{93\ \text{eV}}. \tag{1}$$

On the other hand, sterile neutrinos could possess the right features to solve the DM problem and play some role in neutrino mass generation.[1] This is particularly true in the model of Ref. [10]. There the authors managed to get a realistic model for neutrino mass by adding right-handed neutrinos and scalar multiplets in such a way to obtain small neutrino masses and provide a scenario for leptogenesis. The interesting thing is that one of these neutrinos is sterile and stable and could be a DM candidate. Another such link between DM and sterile neutrinos is provided in Ref. [11], where a version of a left-right symmetric model is extended with a $U(1)$ gauge symmetry. Using some nonsupersymmetric R-parity symmetry, the authors get a stable neutrino interacting with an electron and a charged scalar and analyze its viability as a DM candidate. In such a model there is no tree-level direct detection constraint since the interaction is leptophilic. We refer to a third model where such a sterile neutrino would appear, the so-called $3-3-1\text{RH}_\nu$ model. It is a gauge extension of the SM from $SU_L(2)\otimes U_Y(1)$ to $SU_L(3)\otimes U_N(1)$ with right-handed neutrinos as part of a fundamental representation under $SU_L(3)$ for the leptons [12,13], and when the symmetry is broken to the SM, the lepton triplet decomposes into the usual lepton doublet and a singlet right-handed neutrino under SM symmetry. Besides being capable of generating appropriate neutrino masses [14], among other features that help to tackle unsolved problems of the SM, this $3-3-1$ model possesses at least one scalar that plays the role of a WIMP DM candidate [15].

Inspired by some features of these nonsupersymmetric models [10,11,13], we propose a simple effective low energy model for a DM singlet Majorana fermion. We suppose the presence of a right-handed singlet fermion, which reveals itself to be sterile under electroweak interactions, a sterile Majorana fermion (SMF), and two singlet scalars, a neutral and a charged one. The role of the neutral and charged scalars is to give a mass to the SMF and to add an important channel that contributes to the DM abundance, respectively. It is through the charged scalar-SMF-charged lepton coupling that we will have some control on the SMF abundance. We restrict this lepton to be the electron for simplicity, though it could be extended to

*cpires@fisica.ufpb.br
†farinaldo@fisica.ufpb.br
‡psilva@fisica.ufpb.br

[1]There are some interesting studies in the literature where sterile neutrinos are at the keV scale; see, for example, Ref. [9], constituting a warm DM candidate. We are not going to pursue this possibility in this work.

muon and/or tau leptons. In this way, our model could be seen as part of a low energy limit of the models mentioned above [10,11,13], emphasizing that some larger scheme can be introduced to justify our approach. We observe that, as our SMF does not mix with active neutrinos, direct detection may be its only connection with electroweak physics. This is at variance with usual sterile neutrinos in the literature, where sterile neutrinos are introduced in the context where there is some amount of mixing with active ones, which is severely constrained by big bang nucleosynthesis [16].

Among the recent direct detection experiments, CoGeNT and CDMS-II reported excess events which could be interpreted as a WIMP signal [3,5]. The DAMA Collaboration, that detected an annual modulation in the rates of nuclear recoil, has also claimed that this modulation is a DM discovery signal [6]. These three experiments altogether seem to favor a light WIMP with mass around a few to tens of GeV. Although they face strong constraints from other experiments, such as XENON100, for instance, there remains the possibility that spin-independent (SI) elastic scattering could explain them, as explored in Refs. [17–19].

Our main purpose in this work is to show that our SMF can provide the appropriate DM content of the Universe according to WMAP [2], for a wide SMF mass range, which also agrees with the latest bounds from direct detection experiments. Then, we consider an explanation to CoGeNT and/or CDMS-II excess events, when interpreted as a DM signal [20], as well as DAMA and study how our results constrain the SMF and Higgs masses.

The paper is organized as follows. In Sec. II, we present our SMF model, identifying the physical fields (mass eigenstates) and imposing the discrete symmetry which makes the SMF stable. Next, in Sec. III, we compute the relic abundance of our WIMP candidate, and in Sec. IV we impose the direct detection bounds, paying some attention to the region of positive signals from CDMS-II, CoGeNT, and DAMA. We finally show our conclusions in Sec. V.

II. STERILE MAJORANA FERMION MODEL

The model consists of a small extension of the SM by including a singlet Majorana fermion N_R plus a singlet charged scalar $\eta^{\pm}$ and a singlet neutral scalar σ. Besides the mixing among the Higgs doublet and the new singlet scalars, there is an interaction term coupling these singlets to the leptons,[2] as can be seen in the following Lagrangian:

$$\mathcal{L} \supset \mathcal{L}_{\mathrm{Kin}} - \lambda_1(\bar{N}_R^c N_R \sigma + \bar{N}_R N_R^c \sigma^*) + \lambda_2(\bar{N}_R^c e_R \eta^+ + \bar{e}_R N_R^c \eta^-) - V'(\phi, \eta^{\pm}, \sigma), \quad (2)$$

[2]We will restrict our analysis to one family of leptons since this will be justified later when considering the embedding of this model in a realistic context considering neutrino mass.

where $\mathcal{L}_{\mathrm{Kin}}$ is the Lagrangian term involving the kinetic terms for the singlet fermion as well as for the singlet scalars, including the $\eta^{\pm}$ interaction with SM gauge bosons Z and γ. From this Lagrangian we observe that the scalars carry two units of lepton number if we admit lepton number conservation (they are called scalar bileptons). Notice also that $\eta^{\pm}$ will have interaction terms with the photon and Z boson, since it possesses nonzero hypercharge. The scalar potential in the above Lagrangian, $V'(\phi, \eta^{\pm}, \sigma)$, embraces the new terms to be added to the SM Higgs potential, in order to form the complete scalar potential $V(\phi, \eta^{\pm}, \sigma) = V'(\phi, \eta^{\pm}, \sigma) + V_{\mathrm{SM}}$, given by

$$\begin{aligned} V(\phi, \eta^{\pm}, \sigma) = {} & m_\phi^2 \phi^\dagger \phi + m_\sigma^2 \sigma^* \sigma + \mu_\eta^2 \eta^+ \eta^- \\ & + \lambda_\phi (\phi^\dagger \phi)^2 + \lambda_\sigma (\sigma^* \sigma)^2 + \lambda_\eta (\eta^+ \eta^-)^2 \\ & + \lambda_3 (\phi^\dagger \phi)(\eta^+ \eta^-) + \lambda_4 \eta^+ \eta^- \sigma^* \sigma \\ & + \lambda_5 \phi^\dagger \phi \sigma^* \sigma, \end{aligned} \quad (3)$$

where the field ϕ represents the usual SM scalar $SU_L(2)$ doublet.

Observe that our Lagrangian [Eq. (2)] allows the presence of some extra terms not included here. For example, we could add a term connecting the lepton doublet $L \equiv (\nu_{eL}, e_L)^T$ with the singlet fermion through the SM scalar doublet $\bar{L}\tilde{\phi} N_R + \mathrm{H.c.}$, where $\tilde{\phi} \equiv \imath\sigma_2 \phi^*$. This term would imply a coupling and mixing of the singlet fermion with standard left-handed neutrinos and possibly its decay. However, we want to avoid such terms since we are interested in explaining the DM component as constituted by the singlet fermion even when it is relatively heavy. We choose to get rid of these kind of couplings by assigning a discrete Z_2 symmetry to the model so that N_R and $\eta^{\pm}$ transform as

$$(N_R, \eta^+) \rightarrow (-N_R, -\eta^+), \quad (4)$$

while the remaining fields are even under this symmetry. That is what makes this singlet fermion a sterile one, the SMF, in the sense that it does not couple to any gauge boson of the SM and would leave no sign of its existence through the known interactions; for example, it does not contribute to the invisible width of the Z boson. For that reason we can make this SMF as light as we wish (around 10 GeV in our case). This model is what we call a leptophilic model for the charged scalar in the sense that it does not mediate any interaction involving quarks. Even if we had enforced this scalar to couple to some quark, this one should be an exotic quark, meaning that it would carry lepton number and be a bilepton, too, if we want to preserve lepton symmetry from being broken explicitly. These kinds of particles, scalar and quark bileptons, are very common in the class of models called $3-3-1$ [13,21], and a neutral scalar bilepton was already pointed as a WIMP DM candidate in a version of $3-3-1$ with right-handed neutrinos in the fundamental triplet representation [15].

In this work we rely on the possibility that some high energy fundamental theory is going to generate this effective model properly. In this way we consider the charged scalar mass scale as a free parameter in the range of 100 GeV–3 TeV. Meanwhile, the SMF mass can be generated by spontaneous symmetry breaking due to a nonzero vacuum expectation value acquired by σ, v_σ, which we suppose to be real and assuming values from hundreds of GeV to TeV scale:

$$\sigma = \frac{1}{\sqrt{2}}(v_\sigma + R_\sigma + iI_\sigma). \tag{5}$$

A Majoron should emerge from this breaking mechanism, but it turns out to be a safe Majoron since it does not couple to the electroweak sector except for the Higgs, putting us in a comfortable situation to not worry about its presence in the spectrum. Then, from Eq. (2), we can naturally have a SMF mass in the range of a few to hundreds of GeV:

$$M_N = \lambda_1 v_\sigma \sqrt{2}. \tag{6}$$

Issues concerning light neutrino masses can be addressed by different approaches developed in Refs. [10,11,13], which seem to be particularly interesting to embed our model. We noticed that our SMF mimics the couplings with a neutral singlet scalar and/or the charged singlet scalar in their models. The models in Refs. [10,11] have already proposed that there is a stable right-handed neutrino in their spectra, although they did not deeply survey this possibility as we are going to do here. In the case of the model in Ref. [11], which we can recover when σ decouples, the authors point out the limitation that their neutrino does not give a sign in direct detection experiments. Also, for the case where the charged scalar is almost degenerate in mass with the neutrino, it is fair to mention that coannihilation plays an important role, changing a little their quantitative results, though it does not really change their qualitative aspects. As for the case of the model in Ref. [10], a complete analysis of abundance and direct detection is lacking. Even if we cannot directly compare our results, it has an appropriate frame to embed our model, since our SMF is much like their third neutrino—it can be a plausible DM candidate, a WIMP. In fact, our proposed charged current involves a SMF and the electron, instead of a heavier lepton. We could impose a coupling to a heavier charged lepton, muon, or tau, but we do not expect big quantitative differences concerning these alternative choices, though, and will keep the coupling with the electron only, recovering the main aspects of their DM sector when $\eta^\pm$ decouples. In what concerns the $3-3-1$ model [12,13], the possibility of a right-handed neutrino as a DM candidate is still under study, and again we have no direct way to contrast results.

As we mentioned above, our SMF does not have to obey the mass bounds on the direct production of neutral fermions through Z boson invisible decay, and we can safely have $M_N < M_Z/2$. As for the charged scalar bilepton, we will take its mass above 100 GeV [22], although we allow for lower masses when considering DAMA and CoGeNT results, since deeper studies have to be pursued in order to establish the right lower bound on this scalar mass in this model. We will also obey the Higgs mass lower bound imposed by LEPII, $M_H \geq 114.4$ GeV [22]. The new Yukawa couplings will be fixed by taking the SMF mass and charged scalar mass as free parameters, while the couplings in the scalar potential will be considered close to unit.

Scalar mass spectrum

The scalar masses can be obtained by diagonalizing the mass matrix from the potential equation (3). We take the basis for the real part of neutral scalars, R_ϕ and R_σ, resulting in the following mass matrix:

$$M^2 = \begin{pmatrix} \lambda_\phi v_\phi^2 & \frac{\lambda_5}{2} v_\sigma v_\phi \\ \frac{\lambda_5}{2} v_\sigma v_\phi & \lambda_\sigma v_\sigma^2 \end{pmatrix}, \tag{7}$$

which was obtained after using the minimum conditions for the scalar potential:

$$\begin{aligned} \mu_\sigma^2 + \lambda_\sigma v_\sigma^2 + \frac{\lambda_5}{2} v_\phi^2 &= 0, \\ \mu_\phi^2 + \lambda_\phi v_\phi^2 + \frac{\lambda_5}{2} v_\sigma^2 &= 0. \end{aligned} \tag{8}$$

As for the pseudoscalars, those coming from the Higgs doublet play the same role as before, providing the usual Goldstone bosons for the SM, while the new pseudoscalar coming from the singlet neutral scalar becomes a massless Majoron, $I_\sigma \equiv J$, which does not couple to the electroweak sector except through the standard Higgs boson. We keep it massless throughout this work, though it could get a mass from effective operators or radiative corrections and still be a light particle, not changing our results. Of course, it can be a DM candidate, too, but a nonthermal one, and we are not going to analyze this possibility here.

The mass matrix [Eq. (7)] can be easily diagonalized to give the following mass eigenvalues:

$$\begin{aligned} M_H^2 &= \lambda_\sigma v_\sigma^2 + \lambda_\phi v_\phi^2 \\ &\quad - \sqrt{\lambda_\sigma^2 v_\sigma^4 + \lambda_5^2 v_\phi^2 v_\sigma^2 - 2\lambda_\sigma \lambda_\phi v_\phi^2 v_\sigma^2 + \lambda_\phi^2 v_\phi^4}, \\ M_{\sigma^0}^2 &= \lambda_\sigma v_\sigma^2 + \lambda_\phi v_\phi^2 \\ &\quad + \sqrt{\lambda_\sigma^2 v_\sigma^4 + \lambda_5^2 v_\phi^2 v_\sigma^2 - 2\lambda_\sigma \lambda_\phi v_\phi^2 v_\sigma^2 + \lambda_\phi^2 v_\phi^4}, \end{aligned} \tag{9}$$

with the respective approximate mass eigenstates, the Higgs and the new neutral scalar:

$$H = \frac{1}{\sqrt{1+(\frac{\lambda_5 v_\phi}{2\lambda_\sigma v_\sigma})^2}}\left(R_\phi - \frac{\lambda_5 v_\phi}{2\lambda_\sigma v_\sigma} R_\sigma\right),$$
$$\sigma^0 = -\frac{1}{\sqrt{1+(\frac{\lambda_5 v_\phi}{2\lambda_\sigma v_\sigma})^2}}\left(R_\sigma + \frac{\lambda_5 v_\phi}{2\lambda_\sigma v_\sigma} R_\phi\right). \quad (10)$$

Observe that our model resembles a model for a singlet Dirac neutrino as a DM candidate [23], but theirs strongly differs from ours since their model allows for a Higgs heavier than the neutral scalar by changing the parameters without changing the respective eigenstates. Here the Higgs is always lighter than the neutral scalar once it is given mostly by the first combination in Eq. (10), and no change in parameters can change the relation between the masses in Eq. (9) without changing the eigenstates in Eq. (10).

Finally, the charged scalar bilepton $\eta^\pm$ has a mass term given by

$$m_\eta^2 = \mu_\eta^2 + \frac{\lambda_4}{2} v_\sigma^2 + \frac{\lambda_3}{2} v_\phi^2, \quad (11)$$

which can be considered as a free parameter since μ_η is unknown and can assume any value. We will always take this mass value bigger than the SMF mass in order to guarantee the SMF stability. Next we analyze the viability of the SMF as a WIMP DM candidate by computing its relic abundance and direct detection signals.

III. WIMP RELIC ABUNDANCE

Based on the previous discussion, the neutral stable particle of this model which plays the role of a WIMP is the SMF, which is sterile under electroweak interactions. Its stability is guaranteed by a discrete symmetry (the Z_2 symmetry defined in Sec. II) which avoids its coupling to left-handed neutrinos, while its mass is less than the new charged singlet scalar. However, it must reproduce the right relic abundance, $\Omega_{\rm DM} \simeq 22\%$, and at the same time it cannot conflict with established direct detection experiments [3,4]. Let us first consider the computation of its relic density.

We assume that the SMF was in thermal equilibrium with the SM particles until its decoupling from the thermal bath, the freeze-out epoch. This thermal equilibrium is possible thanks to the interaction between the SMF and the electron and also to the Higgs boson, due to its mixing with the neutral scalar singlet in Eq. (10). Since we are talking about a WIMP, the freeze-out temperature is reached when it is nonrelativistic, meaning that the energy scale to be considered is about $M_N/20$, where M_N is the SMF mass. We can then follow the evolution of the particle number density n through the Boltzmann equation while the Universe undergoes its expansion:

$$\frac{dn}{dt} + 3Hn = -\langle\sigma v_r\rangle(n^2 - n_{\rm eq}^2), \quad (12)$$

where H is the Hubble parameter, which can be written as $H^2 = 8\pi\rho/3M_{\rm Pl}^2$ for a flat universe, $\langle\sigma v_r\rangle$ is the WIMP annihilation cross section thermally averaged with the relative velocity v_r, and $n_{\rm eq}$ is the particle number density at equilibrium. In the expression for the Hubble parameter, $M_{\rm Pl} \approx 1 \times 10^{19}$ GeV, which is the Planck scale, and ρ is the energy density of the Universe. Since WIMPs are intrinsically nonrelativistic at the time of decoupling ($T \ll M_N$ in our case), its equilibrium number density is given by the quantum statistical mechanics expression

$$n_{\rm eq} = g_N\left(\frac{M_N T}{2\pi}\right)^{3/2} e^{-(M_N/T)}, \quad (13)$$

where g_N refers to the WIMP internal degrees of freedom. In general, we follow the standard procedure derived in Refs. [1,24] by defining $x \equiv M_N/T$ and using the nonrelativistic approximation for the squared center of momentum energy, $s = 4M_N^2 + M_N^2 v_r^2$, to expand the thermally averaged cross section until the first power in v_r^2, which allows us to write it as

$$\langle\sigma v_r\rangle \approx a + \frac{6b}{x}, \quad (14)$$

where a and b are the model-dependent parameters. Then we can write the approximate relic WIMP abundance as

$$\Omega_N h^2 \approx \frac{1.04 \times 10^9}{M_{\rm Pl}} \frac{x_F}{\sqrt{g^*}(a + \frac{3b}{x_F})}, \quad (15)$$

where x_F is $x \equiv M_N/T$ computed at the WIMP decoupling temperature given by

$$x_F = \ln\left[c(c+2)\sqrt{\frac{45}{8}}\frac{g_N}{2\pi^3}\frac{M_N M_{\rm Pl}(a + \frac{6b}{x_F})}{\sqrt{g^* x_F}}\right], \quad (16)$$

which, according to what was mentioned before, is generally close to $x_F \approx 20$. In this expression, g^* is the number of degrees of freedom of all relativistic SM particles in thermal equilibrium with the WIMP at freeze-out temperature, which depends on the number of SM channels accessible at such temperature, with $g_N = 2$ in our case, while the constant c is taken to be of the order of 1. The exact value of this constant is unimportant since it has only a small effect in the logarithmic dependence of x_F.

In a first naive approximation we could solve Eq. (16) iteratively and plug the result in Eq. (15), by considering the annihilation channel $N + N \to X + Y$, where X and Y can be any SM particle or even the light singlet scalars of the model (see Fig. 1).

Nevertheless, considering only those Feynman diagrams in Fig. 1, while giving a rough estimate of Ω_N, would not be appropriate for all regions of the available parameter space. Many coannihilation channels would be important when $M_\eta \simeq M_N$ (see some of the coannihilation contributions in Fig. 2). We stress that in some regions of parameter space, even a 100 GeV mass difference can lead

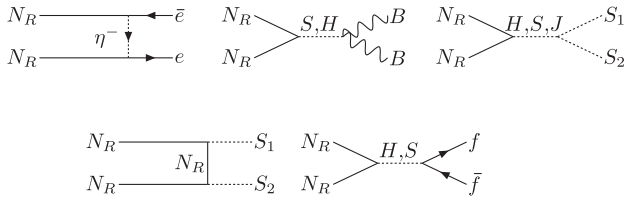

FIG. 1. SMF annihilation channels that contribute to Ω_N. In these graphs, B stands for a $W^\pm$ or a Z gauge boson, S_1 and S_2 represent any possible combination of scalars in the model, H, S, and J, and f is a fermion.

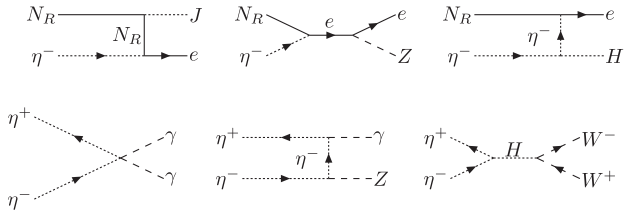

FIG. 2. Some coannihilation channels that contribute to Ω_N.

to significant contributions to Ω_N from these channels. Given the large number of channels that contribute to the abundance, and considering coannihilation, we need to solve the Boltzmann equation numerically. This is done for the exact Boltzmann equation by using the MICROMEGAS package [25], which accurately takes the coannihilation channels into account whenever they are necessary. The Feynman rules used in MICROMEGAS were generated by using the LANHEP package [26]. It is important to emphasize that depending on the SMF mass some of the above diagrams will not take place, since some channels will not be energetically available, which happens when we take sterile fermion masses around 10 GeV.

Next we present our results for the DM relic abundance when the sterile fermion mass is bigger than 50 GeV and separately for a lighter sterile fermion that will be relevant when discussing DAMA, CoGeNT, and CDMS-II positive signals in Sec. V.

A. DM abundance for $M_N \geq 50$ GeV

In order to estimate the contribution of the sterile fermion to the DM relic abundance, it is necessary to make some assumptions on the parameter space of the model. This sterile fermion model has quite a number of free parameters besides those of the SM. There is one vacuum expectation value for the neutral singlet scalar, v_σ, which we suppose to be larger than or equal to 500 GeV since it has to be related to new physics at a high energy scale, eight coupling constants from the fermionic sector and the scalar potential, and the charged singlet scalar mass. We try to avoid fine-tuning whenever possible, so that the coupling constants are of the order of 1. Also, we want the model to be testable at LHC, so we impose that mass scales are at most 1 TeV.[3] Concerning the experimental results on DM relic abundance, we consider in this work the WMAP results with 95% C.L. [2], namely, $0.108 \leq \Omega_{\rm DM}h^2 \leq 0.121$. With these basic assumptions we have made some quantitative predictions for the relic density of this SMF in some specific regimes of the model proposed above.

We first compute the relic density for several points in the parameter space, for couplings varying about 0.1, a sterile fermion mass between $M_N = 50$ GeV and $M_N = 1$ TeV, and a range of Higgs mass between $M_H = 114.4$ GeV and $M_H = 300$ GeV. We consider two cases: one without coannihilation with $\eta^\pm$ and another including the coannihilation. For the first case we suppose a mass difference between the sterile fermion and charged scalar of 100 GeV. In the second case, such a difference is only of the order of 10 GeV, except when we have sterile fermion masses less than 90 GeV, since we maintain the charged scalar heavier than 100 GeV. In Fig. 3, we show a scatter plot for the relic abundance in terms of the sterile fermion mass without and with coannihilation. This figure shows that coannihilation is not determinant to have compatible models of sterile fermions as a viable DM candidate, but it clearly fills much more of the parameter space than the case without coannihilation. Just as an illustration we also show in Fig. 4 the relic abundance when the Higgs mass is fixed in two cases: one for $M_H = 115$ GeV and the other for $M_H = 300$ GeV. In this case both graphs include coannihilation. There is almost no quantitative difference in the relic abundance concerning the difference in Higgs mass within the range $114.4\ \text{GeV} \leq M_H \leq 300$ GeV.

It is also interesting to consider two limit situations for this model: one in which the neutral scalar decouples from the spectrum and another one in which the charged scalar is the decoupling particle. The first situation is a peculiar one in the sense that no direct detection experiment is available to test it (if radiatively induced N_R-quark couplings are irrelevant), since in such a case there is no mediator particle that could connect the WIMP with the nuclei. Only accelerator experiments can put a constraint on it, unless a signal is confirmed by current direct detection experiments, which would leave no room for this possibility. On the other hand, the absence of any direct detection signal would favor such a possibility. We show in Fig. 5 the results for the relic abundance in these situations for Higgs mass varying between $114.4\ \text{GeV} \leq M_H \leq 300$ GeV. The first panel is for the σ^0-less model with coannihilation, and the second panel is for the $\eta^\pm$-less model which has no coannihilation channel. From these figures we notice that a SMF can be the whole DM in both situations for many points in the parameter space, and

[3]An exception will be made when we treat the case where $M_N \leq 50$ GeV, where we allow for $m_{\eta^\pm}$ to be as high as 3 TeV and even bigger, allowing for $\eta^\pm$ decoupling.

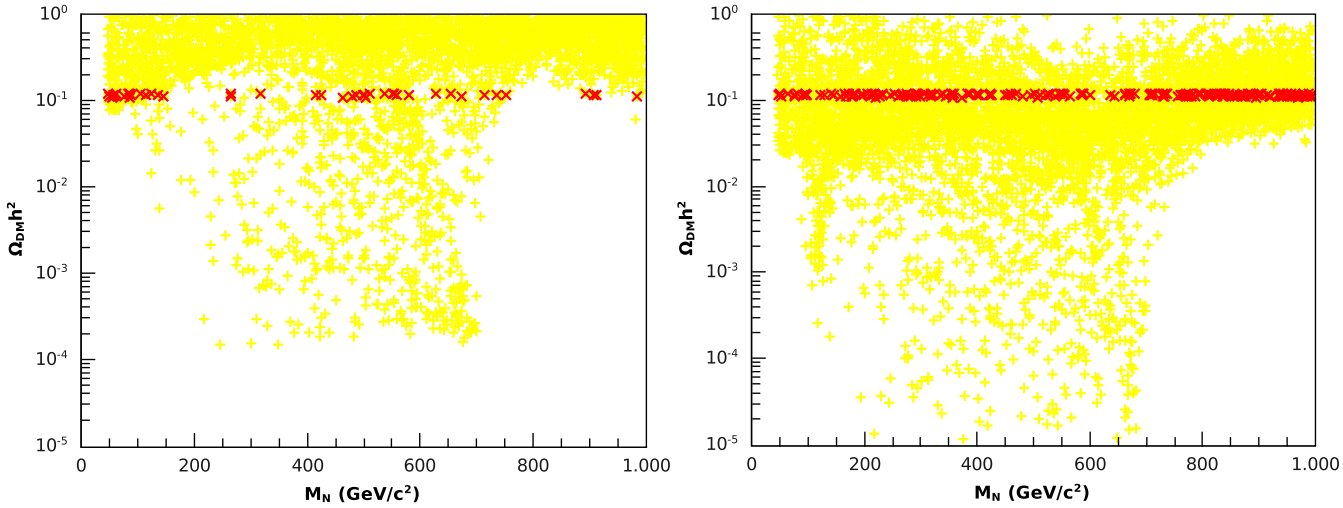

FIG. 3 (color online). Scatter plot for the relic abundance as a function of sterile fermion mass. The left panel was computed without coannihilation, while the right panel includes coannihilation. In these graphs the yellow cross represents points for several possible outcomes for the model considered, while the red cross represents only those points in parameter space which are in agreement with WMAP within 95% C.L.

the case with no $\eta^{\pm}$ is preferred only if any direct detection signal is claimed, a possibility we are going to treat in Sec. IV. In any case, if for some reason, nature chooses a scenario for the realization of this model which is not strictly the one with both $\eta^{\pm}$ and σ^0 in the low energy spectrum, which means that one of them would decouple, it is interesting to check that these two situations do not describe the same physics and hence they are inequivalent and distinguishable.

B. DM abundance for $M_N \leq 50$ GeV

Here we specialize to the situation where the neutrino mass is relatively small because, as we will see in the next section, there are three recent direct detection experiments [3,5,6] that allow for a positive signal for a WIMP mass lower than 50 GeV, and we consider this possibility from now on. In order to convey an explanation for these signals in our model, we have to make different assumptions on some values of its parameters. The Higgs and the charged scalar mass will be free to vary from 115 GeV $< M_H <$ 300 GeV and $m_\eta \geq 500$ GeV. Below, in Fig. 6, we show the abundance for the SMF in separate panels. The first panel concerns the region of WIMP mass favored by DAMA and CoGeNT, which is around $M_N \approx 10$ GeV, and the second panel presents the mass range favored by CDMS-II, 20 GeV $< M_N <$ 50 GeV.

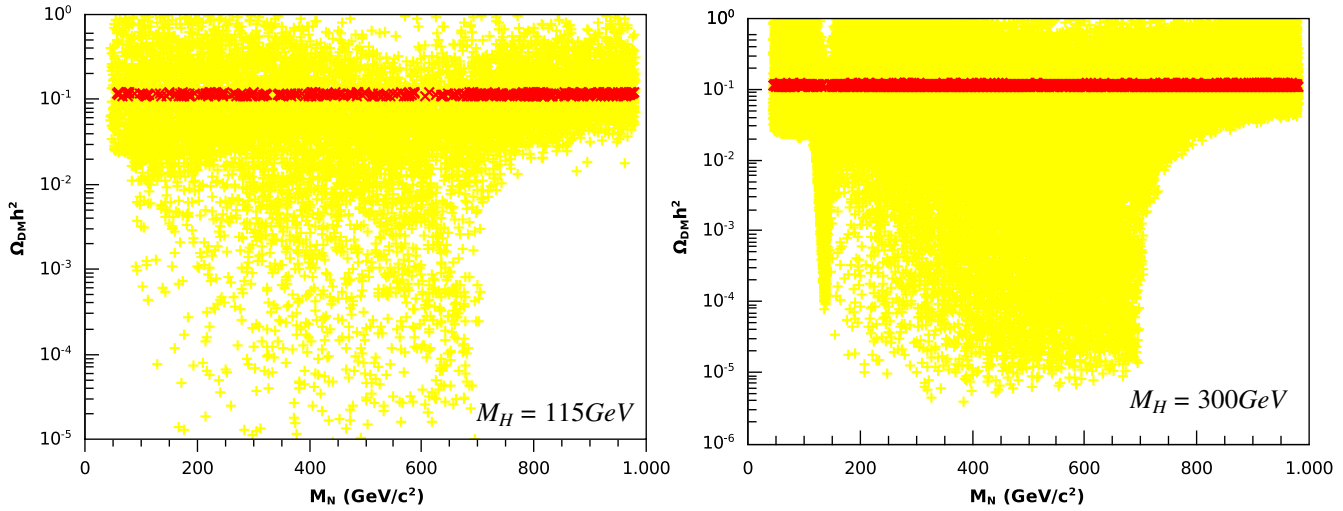

FIG. 4 (color online). Scatter plot for the relic abundance as a function of SMF mass for a Higgs mass of 115 (left panel) and 300 GeV (right panel), with coannihilation. The yellow cross represents points for several possible outcomes for the model considered, while the red cross represents only those points in parameter space which are in agreement with WMAP within 95% C.L.

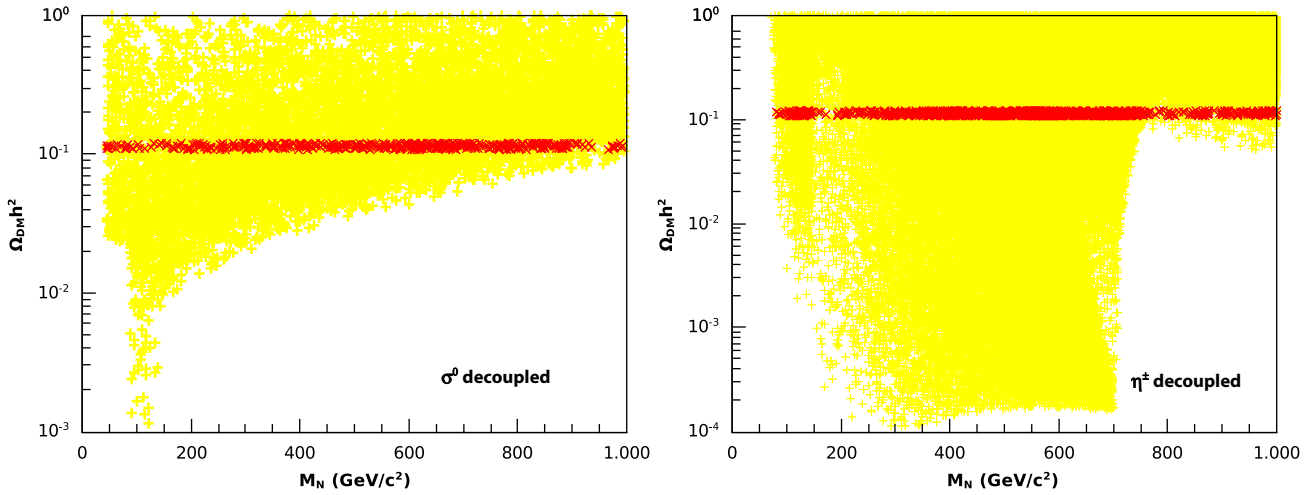

FIG. 5 (color online). Scatter plot for the relic abundance as a function of SMF mass. The left panel corresponds to the model without σ^0, while the right panel refers to the model without $\eta^{\pm}$. The yellow cross represents points for several possible outcomes for the model considered, while the red cross represents those points in parameter space which are in agreement with WMAP within 95% C.L.

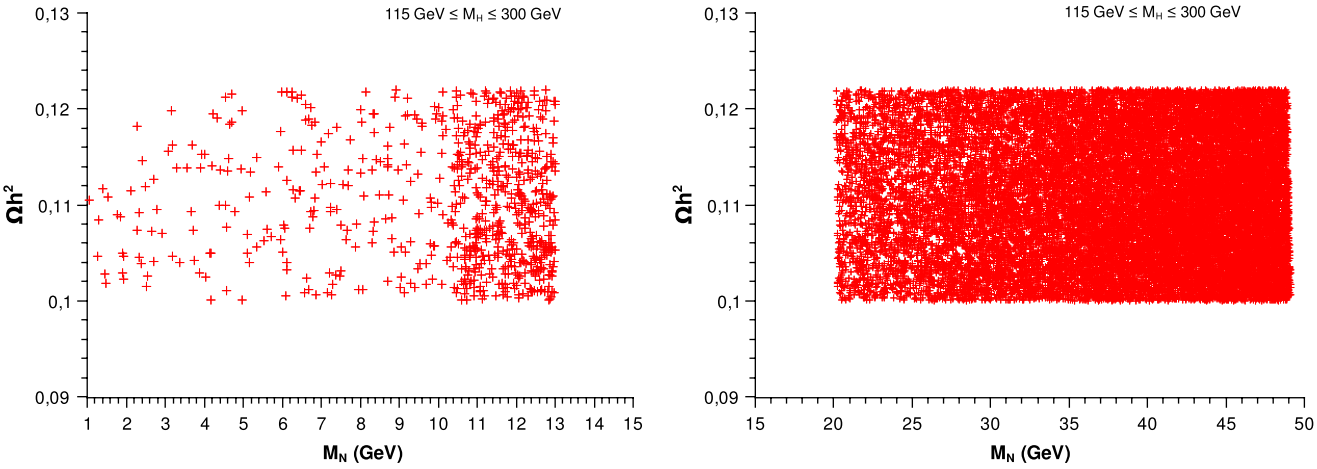

FIG. 6 (color online). Relic abundance for the SMF lighter than 50 GeV. The left panel corresponds to the abundance of the SMF for the range of masses favored by DAMA and CoGeNT with $\eta^{\pm}$ decoupled, while the right panel is for the mass range favored by CDMS-II and $m_\eta < 3$ TeV. Both are in agreement with WMAP within 95% C.L.

The left panel was obtained by decoupling the $\eta^{\pm}$ from the spectrum, assuming its mass much bigger than 3 TeV. In the right panel, we varied the $\eta^{\pm}$ mass from 500 GeV $< M\eta <$ 3 TeV. These choices were made because they give us the best results for the WIMP-nucleon cross section that will be discussed in the next section. We have to remark that we were unable to obey WMAP constraints for Higgs masses bigger than our upper limit $M_H = 300$ GeV, meaning that a light Higgs is preferred in this scenario.

We have shown in this section that our SMF can account for the whole DM content of the Universe for a wide range of reasonable values for the parameter space and neutrino masses from 10 GeV $\leq M_N \leq$ 1 TeV. Next we are going to investigate the compatibility of our model concerning the bounds imposed by direct detection experiments and also seek an explanation for CoGeNT and/or CDMS-II excess events and DAMA annual modulation signal.

IV. DIRECT DETECTION

The direct detection method of DM relies on the idea of measuring the nuclear recoil energy deposited by an incident WIMP into a target nucleus which composes an underground experiment. For a given model we can follow the standard procedure in order to get the WIMP-nucleon coupling (see Ref. [25]) and after that write the WIMP-nucleus cross section at zero momentum transfer [1,25,27]:

$$\sigma_0 = \frac{4\mu_r^2}{\pi}(Zf_p + (A - Z)f_n)^2, \tag{17}$$

where $\mu_r = M_N m_A/(M_N + m_A)$ is the reduced WIMP mass, m_A the nucleus mass, Z the atomic number, and A the atomic mass.

It is important to emphasize some properties of this interaction. First, as the energy of the incident WIMP is low, the wavelength of the WIMP is comparable to or larger than the size of the nucleus; therefore the WIMP interacts with the nucleus coherently. Second, in most instances $f_p \cong f_n$, the WIMP-nucleus cross section has a squared A dependence, and hence heavier nuclei are preferred to search for scalar interactions. Since the DM direct detection experiments contain nuclei with different atomic masses, we need to define the so-called WIMP-nucleon cross section in order to compare the results among different experiments. This can be written as

$$\sigma_{p,n}^{\mathrm{SI}} = \sigma_0 \frac{\mu_{p,n}^2}{\mu_r^2 A^2}, \tag{18}$$

where $\mu_{p,n}$ is the proton or neutron-WIMP reduced mass.

Several experiments have been looking for a WIMP signal; nevertheless, almost all of them have reported only null results, although imposing strong limits in this WIMP-nucleon cross section for a wide range of masses. Nevertheless, it is fair to mention that the DAMA Collaboration reported an annual modulation in its event rate with 8.9σ significance [6], and, recently, CDMS-II and CoGeNT germanium detectors observed events in excess which could be interpreted as a WIMP signal [3,5]. Then, for those regions which are compatible with WMAP results, we are going to investigate if our model can satisfy the most recent experimental bounds on the WIMP-nucleon cross section and seek to reproduce the DAMA signal and the excess events detected by CoGeNT or explain the CDMS-II candidate events. Again, to accomplish this task, we are going to use MICROMEGAS [25] to make the numerical computations, whose results we present next.

A. Direct detection for $M_N \geq 50$ GeV

Below (see Fig. 7) we show the results for the case where $\eta^{\pm}$ and σ^0 are present in the spectrum. In all of the following figures concerning DM direct detection, we used experimental data obtained from the Web site in Ref. [28]. The contours are upper bounds on the elastic SI WIMP-nucleon cross sections, meaning that the region above these contours is experimentally excluded (except for the projected sensitivities of future experiments). From these plots we could say that the heavy SMF is still to be found on direct detection experiments and there is not much qualitative difference if there is or there is not coannihilation, although coannihilation provides a much larger assessable region of the parameter space that can be tested in the near future. We also included plots for two different Higgs mass values: $M_H = 115$ GeV and $M_H = 300$ GeV; see Fig. 8. In these plots we consider only the case where there is coannihilation since it offers a larger testable region of the parameter space. It is noticeable that larger Higgs masses lead to less constrained parameter space, which is easy to understand since the WIMP-quark interaction in this model is due to Higgs exchange and larger Higgs masses have suppressed nuclei

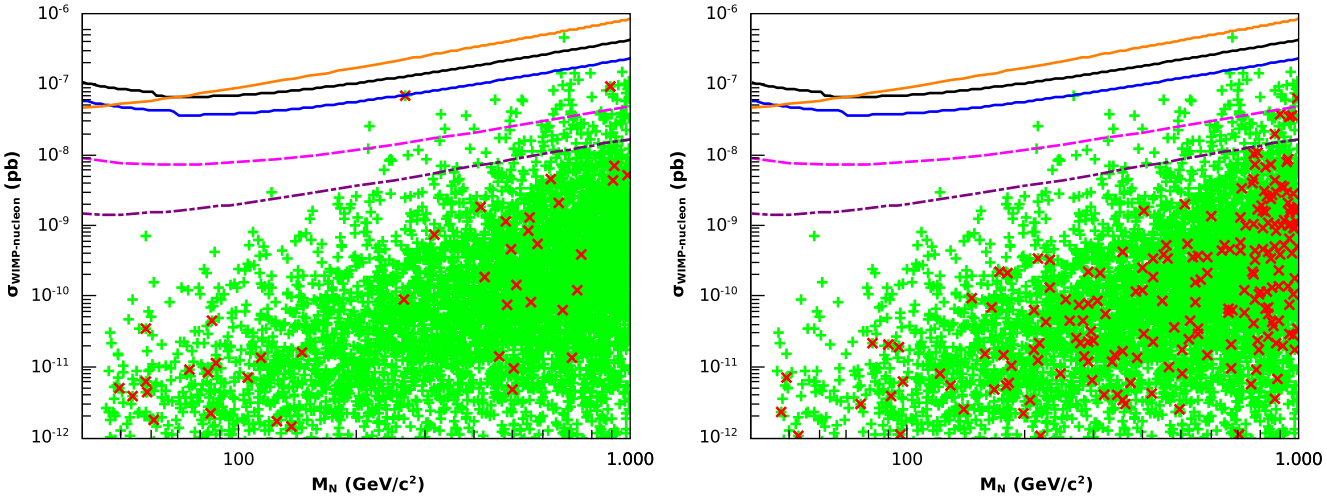

FIG. 7 (color online). Scatter plot for WIMP-proton cross section as a function of SMF mass. The left panel corresponds to the complete model without coannihilation, while the right panel refers to the model with coannihilation. The green cross (+) represents points for several possible outcomes for the model considered, while the red cross (×) represents those points in parameter space which are in agreement with WMAP within 95% C.L. From top to bottom starting at the upper right, the full lines are experimental results: CDMS-II (black), CDMS 2004–2009 combined (blue), and XENON10 (orange); the dashed line (magenta) is CDMS 2ST @ soudan prospect; and the dashed-dotted line (violet) is XENON100 6000 kg prospect.

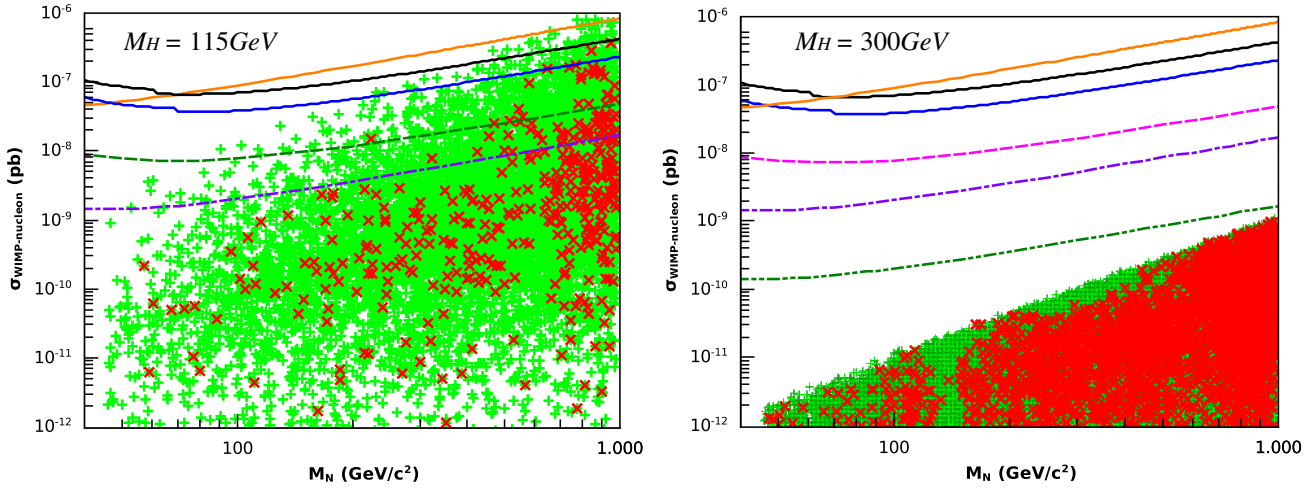

FIG. 8 (color online). Scatter plot for WIMP-proton cross section as a function of SMF mass (with $\eta^{\pm}$ and σ in the spectrum). The left panel corresponds to $M_H = 115$ GeV, while the right panel refers to the model with $M_H = 300$ GeV. The green cross (+) represents points for several possible outcomes for the model considered, while the red cross (×) represents those points in parameter space which are in agreement with WMAP within 95% C.L. From top to bottom starting at the upper right, the full lines are experimental results: CDMS-II (black), CDMS 2004–2009 combined (blue), and XENON-10 (orange); the dashed line (magenta) is CDMS 2ST @ soudan prospect; and the dashed-dotted line (violet) is XENON100 6000 kg prospect. In the right panel we included XENON-100 60000 kg prospect as a dashed-double dotted line (olive).

cross sections. We added a future prospect experiment, XENON 60000 kg, in the second panel of Fig. 8, to stress the fact that the model with large M_H is still far from being probed. When $M_H = 115$ GeV, only a few points above $M_N \approx 600$ GeV are excluded and most of the parameter space is in a safe region and can be assessed in the near future.

B. DAMA, CDMS-II, and CoGeNT positive signals

The DAMA Collaboration, which has collected over 1.17 ton-years of data, reported an annual modulation in their event rate with 8.9σ significance [6]. Such a signal arises naturally from postulating WIMPs in the Galactic halo that scatter off target nuclei in the detectors, and, since no background source was identified that could explain this modulation, the signal was interpreted as evidence of DM. The parameter space favored by DAMA is essentially excluded by other experiments; however, implications of new effects in NaI crystals, namely, channeling [29], have been used in order to evade the exclusion limits [30].

Recently, the CDMS Collaboration has reported its results of the final data runs of the CDMS-II and observed that two candidate events have survived after application of many discrimination procedures [3]. The probability to observe two or more background events is 23%, which means that the two events neither provide statistically significant evidence for DM nor can be rejected as background. Therefore many works have been done interpreting these two candidates events as a WIMP signal [31].

Another excess of events was also observed by the CoGeNT Collaboration. CoGeNT is an ultralow noise germanium detector that over a period of 56 days reported approximately 100 events which are consistent with a WIMP nuclear recoil. Such a WIMP is constrained to have a mass in the 7–12 GeV range and an elastic scattering cross section: $\sigma \cong 7 \times 10^{-41}$ cm^2. Since CoGeNT does not distinguish nuclear from electron recoils, it is reasonable to take the confidence interval for CoGeNT data for 30% and 50% exponential background contribution.

The parameter space favored by the CDMS-II and CoGeNT experiments are distinct, and hence we will study if the model can either explain CDMS-II or CoGeNT signals. Although the cross section required to explain the DAMA signal without any channeling is too high to explain CoGeNT, while DAMA with 100% channeling is too low, some consistency between them can be found through appropriate choices of the halo model and the fraction of channeled events in DAMA [17–19,32], with

$$10^{-4}\ \text{pb} \leq \sigma_{\text{WIMP-nucleon}} \leq 10^{-5}\ \text{pb}. \qquad (19)$$

In this sense we will explore the situation in which CDMS-II and DAMA/CoGeNT signals can be explained separately.

The DAMA, CDMS-II, and CoGeNT favored regions are largely constrained by XENON bounds which recently achieved a low threshold of 2 keV (see Refs. [18,20]). However, there are reasons to be wary, first because by choosing proper background contribution and halo models, the tension with XENON bounds can be diminished and second because the XENON bounds depend on the scintillation efficiency factor L_{eff} for which there is

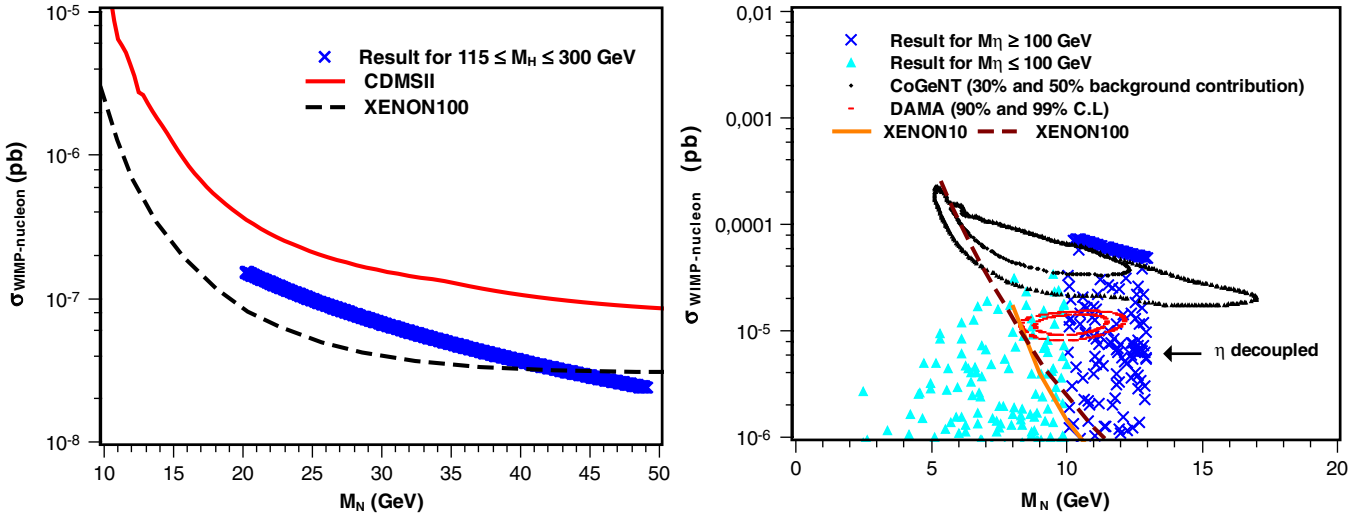

FIG. 9 (color online). In the left panel the blue crosses are the model results, the red curve is from CDMS-II, and the black dashed curve is from XENON-100. In the right panel the magenta triangles are the model results for $M_\eta < 100$ GeV, the blue crosses are the results for $M_\eta \geq 500$ GeV (the denser region involves masses in the range 500 GeV $\leq M_\eta \leq 2$ TeV, and the points below this region represent $M_\eta > 2$ TeV), and the black contours are the CoGeNT favored regions for 30% and 50% background contributions. The red contours are the favored DAMA region 90% and 99% C.L. assuming 100% of channeling. Also shown are XENON10 (orange curve) and XENON100 (dark red dashed curve). We used the DAMA and CoGeNT contours obtained by Ref. [19] and exhibited in the first panel of their Fig. 3. All the points in both graphs are in accordance with WMAP within 95% C.L.

considerable uncertainty [33]. To see how precisely the scintillation efficiency of XENON and astrophysical assumptions affect the direct detection limits, we refer the reader to Refs. [18–20,33,34].

Interpreting that CoGeNT events, the DAMA annual modulation, and the two candidate events observed by CDMS-II are due to a WIMP-nucleon elastic scattering, we exhibit in Fig. 9 the SI cross section for the SMF contrasted with these experiments.

In the left panel of this figure, we plot those points in agreement with WMAP for the WIMP mass region favored by CDMS-II candidate events with 500 GeV $< M\eta <$ 3 TeV. We can see that the model provides a parameter space for masses below 50 GeV and a cross section in the $(10^{-7}$–$10^{-8})$ pb range, which is consistent with the two excess events reported by CDMS-II with 78% C.L. [35]. XENON seems to exclude most of the CDMS-II allowed region, but better consistency may be reached if we take into account the remarks on Ref. [33].

In the right panel, we show that for masses larger than 9 GeV some concordance with CoGeNT excess events and DAMA annual modulation is obtained. In this case, if XENON results can be shifted as claimed [33] and an overlapping region exists [32], we expect that our model should fit both experiments at once. It is important to emphasize that we are using different ranges of mass for the charged scalar $\eta^\pm$ on different regions of this plot. Namely, the uppermost points (denser region) were obtained for 500 GeV $< M_\eta < 2$ TeV, while in the intermediate region, consistent with DAMA and CoGeNT, higher masses were used, $M_\eta \gg 2$ TeV ($\eta^\pm$ decoupled) and the region of WIMP masses less than 10 GeV is potentially discarded since $\eta^\pm$ has to be lighter than 100 GeV in contrast with LEP constraints [22], although a deeper analysis should be performed for this particular model. We should mention that 100 GeV $\leq M_\eta \leq$ 500 GeV are not included in these plots because for low WIMP masses these values correspond to points in the parameter space outside the WMAP region. Therefore, the SMF can explain either the two candidate events observed by CDMS-II or the CoGeNT events in excess for 50% background contribution together with DAMA signal, but not all simultaneously. As we mentioned before, our results are sensitive to the Higgs mass, and the SMF that could explain these experiments demands a rather light Higgs boson ($M_H < 300$ GeV) in order to reproduce the correct DM abundance.

V. CONCLUSIONS

We have defined a scenario for physics beyond the SM where a singlet right-handed Majorana fermion is added together with a charged and a neutral singlet scalar. This scenario may represent some low energy regime of gauge or Higgs extensions of the SM [10,11,13]. The right-handed singlet fermion proves to be a stable SMF if a discrete symmetry is assumed and thus represents a good candidate for the DM in the Universe. We have probed the parameter space of this model and found that there are regions where the model is compatible with recent results of WMAP, allowing this SMF to represent the main component of DM. Also, we have tested this model under direct

DM detection experimental bounds and checked that it is mostly safe for a range of SMF mass between $M_N = 50$ GeV and $M_N = 1$ TeV when the Higgs mass is $114.4\ \text{GeV} < M_H < 300$ GeV. However, we noticed that the lowest Higgs masses provide more interesting results in the sense that they can be probed in such DM detection experiments sooner than higher ones for a SMF heavier than 50 GeV.

Finally, when restricting to lower SMF masses we were able to investigate the possibility of fitting the DAMA annual modulation signal, the CoGeNT excess for 50% exponential background contribution, and CDMS-II excess events at 78% C.L., through SI elastic scattering. The results allow us to conclude that, in the light of the interpretation of those signals as positive WIMP detection, our model can explain these experiments but not all simultaneously. DAMA and CoGeNT can be explained concomitantly for $M_N \approx 10$ GeV if XENON bounds can be pushed to the right as claimed in Ref. [33] and an overlapping region exists [32]. Also, in order to get the correct WIMP abundance and a suitable scattering cross section for direct detection experiments, the model is constrained to yield a rather light Higgs boson: $M_H < 300$ GeV. Although it is too soon to claim for irrefutable detection, it is possible that DAMA, CDMS-II, and CoGeNT are pointing to an intriguing interplay among lepton sector physics, the DM problem, and the Higgs search which, hopefully, will be assessed in the forthcoming experiments.

ACKNOWLEDGMENTS

We thank J. K. Mizukoshi for useful discussions. We also thank A. Semenov for valuable information about LANHEP and CALCHEP and A. Pukhov for his prompt help concerning the MICROMEGAS package. The data we used in DAMA, CoGeNT, and CDMS-II plots were kindly provided by Neal Weiner and Itay Yavin, to whom we feel deeply indebted. This research was supported by the Conselho Nacional de Desenvolvimento Científico e Tecnológico (CNPq) (C. A. S. P., F. S. Q., and P. S. R. S.) and Coordenação de aperfeiçoamento de Pessoal de Nível Superior (CAPES) (F. S. Q.).

[1] G. Jungman, M. Kamionkowski, and K. Griest, Phys. Rep. **267**, 195 (1996); G. Bertone, D. Hooper, and J. Silk, Phys. Rep. **405**, 279 (2005); H. Murayama, arXiv:0704.2276.

[2] E. Komatsu *et al.*, Astrophys. J. Suppl. Ser. **180**, 330 (2009).

[3] D. S. Akerib *et al.* (CDMS Collaboration), Phys. Rev. Lett. **96**, 011302 (2006); Z. Ahmed *et al.* (CDMS-II Collaboration), Science **327**, 1619 (2010); P. L. Brink (CDMS-II Collaboration) *et al.*, AIP Conf. Proc. **1182**, 260 (2009); T. Bruch (CDMS Collaboration), AIP Conf. Proc. **957**, 193 (2007); arXiv:1001.3037.

[4] J. Angle *et al.* (XENON Collaboration), Phys. Rev. Lett. **100**, 021303 (2008); E. Aprile *et al.* (XENON Collaboration), arXiv:1001.2834; E. Aprile and L. Baudis (XENON100 Collaboration), Proc. Sci., IDM2008 (2008) 018; M. Schumann (XENON Collaboration), AIP Conf. Proc. **1182**, 272 (2009); E. Aprile *et al.* (XENON Collaboration), Phys. Rev. Lett. **105**, 131302 (2010); XENON100 Collaboration, arXiv:1005.2615.

[5] C. E. Aalseth *et al.* (CoGeNT Collaboration), arXiv:1002.4703v2.

[6] R. Bernabei *et al.*, Eur. Phys. J. C **67**, 39 (2010); J. Phys. Conf. Ser. **203**, 012003 (2010).

[7] L. Evans, New J. Phys. **9**, 335 (2007); A. Hoecker, arXiv:1002.2891.

[8] S. S. Gershtein and Ya. B. Zeldovich, JETP Lett. **4**, 120 (1966); R. Cowsik and J. McClelland, Phys. Rev. Lett. **29**, 669 (1972).

[9] A. D. Dolgov and S. H. Hansen, Astropart. Phys. **16**, 339 (2002); A. Kusenko, Phys. Rev. Lett. **97**, 241301 (2006); T. Asaka, M. Laine, and M. Shaposhnikov, J. High Energy Phys. 01 (2007) 091; M. Shaposhnikov, Nucl. Phys. **B763**, 49 (2007); D. Gorbunov and M. Shaposhnikov, J. High Energy Phys. 10 (2007) 015; F. L. Bezrukov and M. Shaposhnikov, Phys. Lett. B **659**, 703 (2008); S. Khalil and O. Seto, J. Cosmol. Astropart. Phys. 10 (2008) 024; K. Petraki and A. Kusenko, Phys. Rev. D **77**, 065014 (2008); A. Boyarsky, J. Lesgourgues, O. Ruchayskiy, and M. Viel, Phys. Rev. Lett. **102**, 201304 (2009); D. Cogollo, H. Diniz, and C. A. de S. Pires, Phys. Lett. B **677**, 338 (2009).

[10] Pei-Hong Gu, M. Hirsch, U. Sarkar, and J. W. F. Valle, Phys. Rev. D **79**, 033010 (2009).

[11] S. Khalil, H. S. Lee, and E. Ma, Phys. Rev. D **79**, 041701 (R) (2009).

[12] M. Singer, J. W. F. Valle, and J. Schechter, Phys. Rev. D **22**, 738 (1980); J. W. F. Valle and M. Singer, Phys. Rev. D **28**, 540 (1983).

[13] J. C. Montero, F. Pisano, and V. Pleitez, Phys. Rev. D **47**, 2918 (1993); R. Foot, H. N. Long, and T. A. Tran, Phys. Rev. D **50**, R34 (1994); H. N. Long, *ibid.* **54**, 4691 (1996).

[14] Alex G. Dias, C. A. de S. Pires, and P. S. Rodrigues da Silva, Phys. Lett. B **628**, 85 (2005).

[15] C. A. de S. Pires and P. S. Rodrigues da Silva, J. Cosmol. Astropart. Phys. 12 (2007) 012.

[16] A. D. Dolgov and F. L. Villante, Nucl. Phys. **B679**, 261 (2004); F. L. Villante, Nucl. Phys. B, Proc. Suppl. **168**, 37 (2007).

[17] Kyu Jung Bae, Hyung Do Kim, and Seodong Shin, arXiv:1005.5131; Sarah Andreas, Chiara Arina, Thomas Hambye, Fu-Sin Ling, and Michel H. G. Tytgat, Phys. Rev. D **82**, 043522 (2010).

[18] A. Liam Fitzpatrick, Dan Hooper, and Kathryn M. Zurek, Phys. Rev. D **81**, 115005 (2010).

[19] Spencer Chang, Jia Liu, Aaron Pierce, Neal Weiner, and Itay Yavin, J. Cosmol. Astropart. Phys. 08 (2010) 018.
[20] J. Kopp, T. Schwetz, and J. Zupan, J. Cosmol. Astropart. Phys. 02 (2010) 014.
[21] F. Pisano and V. Pleitez, Phys. Rev. D **46**, 410 (1992); P. H. Frampton, Phys. Rev. Lett. **69**, 2889 (1992).
[22] C. Amsler *et al.* (Particle Data Group), Phys. Lett. B **667**, 1 (2008).
[23] Y. G. Kim, K. Y. Lee, and S. Shin, J. High Energy Phys. 05 (2008) 100.
[24] M. Srednicki, R. Watkins, and K. A. Olive, Nucl. Phys. **B310**, 693 (1988).
[25] G. Bélanger, F. Boudjema, A. Pukhov, and A. Semenov, Comput. Phys. Commun. **180**, 747 (2009); **176**, 367 (2007).
[26] A. Semenov, Comput. Phys. Commun. **180**, 431 (2009); **115**, 124 (1998); arXiv:hep-ph/9608488.
[27] P. F. Smith and J. D. Lewin, Phys. Rep. **187**, 203 (1990); Y. Ramachers, Nucl. Phys. B, Proc. Suppl. **118**, 341 (2003); R. J. Gaitskell, Annu. Rev. Nucl. Part. Sci. **54**, 315 (2004); N. J. Spooner, J. Phys. Soc. Jpn. **76**, 111016 (2007); C. L. Shan, arXiv:0707.0488; D. G. Cerdeño and A. M. Green, arXiv:1002.1912.
[28] We have used the plots of current and projected sensitivities to WIMP direct detection obtained from R. Gaitskell and V. Mandic, http://dmtools.brown.edu/.
[29] R. Bernabei *et al.*, Eur. Phys. J. C **53**, 205 (2008); E. M. Drobyshevski, Mod. Phys. Lett. A **23**, 3077 (2008); Nassim Bozorgnia, Graciela B. Gelmini, and Paolo Gondolo, arXiv:1006.3110.
[30] Frank Petriello and Kathryn M. Zurek, J. High Energy Phys. 09 (2008) 047; Jonathan L. Feng, Jason Kumar, and Louis E. Strigari, Phys. Lett. B **670**, 37 (2008); Malcolm Fairbairn and Thomas Schwetz, J. Cosmol. Astropart. Phys. 01 (2009) 037; Yeong Gyun Kim and Seodong Shin, J. High Energy Phys. 05 (2009) 036; B. Feldstein, A. L. Fitzpatrick, E. Katz, and B. Tweedie, J. Cosmol. Astropart. Phys. 03 (2010) 029.
[31] Xiao-Gang He, Tong Li, Xue-Qian Li, Jusak Tandean, and Ho-Chin Tsai, Phys. Lett. B **688**, 332 (2010); A. Bottino, F. Donato, N. Fornengo, and S. Scopel, Phys. Rev. D **81**, 107302 (2010); Junjie Cao, Ken-ichi Hikasa, Wenyu Wang, Jin Min Yang, and Li-Xin Yu, J. High Energy Phys. 07 (2010) 044; Shaaban Khalil, Hye-Sung Lee, and Ernest Ma, Phys. Rev. D **81**, 051702 (2010); Mayumi Aoki, Shinya Kanemura, and Osamu Seto, Phys. Lett. B **685**, 313 (2010); Qing-Hong Cao, Chuan-Ren Chen, Chong Sheng Li, and Hao Zhang, arXiv:0912.4511.
[32] R. Foot, Phys. Lett. B **692**, 65 (2010).
[33] Christopher Savage, Graciela Gelmini, Paolo Gondolo, and Katherine Freese, arXiv:1006.0972v1; Vernon Barger, Mathew McCaskey, and Gabe Shaughnessy, Phys. Rev. D **82**, 035019 (2010); J. I. Collar and D. N. McKinsey, arXiv:1005.0838v3.
[34] Christopher McCabe, Phys. Rev. D **82**, 023530 (2010);
[35] Marco Farina, Duccio Pappadopulo, and Alessandro Strummia, Phys. Lett. B **688**, 329 (2010).